PCCP

PAPER

View Article Online
View Journal | View Issue

Cite this: *Phys. Chem. Chem. Phys.*, 2015, **17**, 13045

To π or not to π – how does methanol dock onto anisole?†

Matthias Heger, Jonas Altnöder, Anja Poblotzki and Martin A. Suhm*

Received 16th March 2015,
Accepted 14th April 2015

DOI: 10.1039/c5cp01545f

www.rsc.org/pccp

Anisole offers two similarly attractive hydrogen bond acceptor sites to an incoming hydrogen bond donor: its oxygen atom and its delocalized π electron system. Electronic structure calculations up to the CCSD(T)/AVTZ level suggest an isoenergetic situation for methanol after harmonic zero point energy correction, within less than 1 kJ mol^{-1}. Linear infrared absorption spectroscopy in the OH stretching fundamental range applied to a cold supersonic jet expansion of anisole and methanol in helium shows that the oxygen binding site is preferred, with about 20 times less π-bonded than O-bonded dimers despite the non-equilibrium collisional environment. Accidental band overlap is ruled out by OH overtone and OD stretching spectroscopy. Furthermore, the diagonal anharmonicity constant of the OH stretching mode is derived from experiment and reaches 80% of the monomer distortion found in the methanol dimer, as expected for a weaker hydrogen bond to the aromatically substituted oxygen. To reconcile these experimental findings with *ab initio* theory, accurate nuclear and electronic structure calculations involving AVQZ basis sets are required. Dispersion-corrected double-hybrid density functional theory provides a less expensive successful structural approach.

1 Introduction

Anisole (methoxybenzene) is one of the best-studied aromatic systems in the gas phase, also in terms of molecular complexes.[1,2] Brutschy *et al.* investigated its water clusters[3,4] and found the first water to bind to the oxygen of anisole in the electronic ground state, whereas Li^+ is predicted to prefer π binding.[5] A secondary water docking minimum with a π bond was initially elusive,[4] but computationally identified later on.[6] However, it does not play a direct role in the large amplitude motion of the water molecule around the anisole oxygen, which even gives rise to an anomalous structural isotope effect.[6,7] In the mixed trimer, two water molecules bridge the anisole plane[8] from the oxygen atom to the π system.[4] The complex between phenol and anisole also opts for the oxygen binding site.[9] For 1,2-dimethoxybenzene,[10] water similarly prefers oxygen coordination. In contrast, indole prefers the π system of furan over the O coordination as a consequence of the stronger delocalization of the oxygen lone pairs in this heterocycle.[11] A close competition between OH–O and OH–π binding sites has recently been reported for 2,3-benzofuran,[12] where it actually leads to a coexistence of the two docking motifs for both water and methanol in supersonic jet expansions. By combining methanol with anisole, there are thus promising ways to influence the docking preferences in one or the other direction using chemical substitution and it makes sense to start with a detailed study of the parent complex.

Based on the full body of experimental findings, it is plausible but far from certain that methanol will prefer the oxygen docking site of anisole. To the best of our knowledge, no microwave, infrared or IR/UV double resonance spectra of this binary complex have been reported so far, whereas its components are very well investigated.[13,14] Also, OH–O and OH–π isomers of methanol complexing the anthracene analog of anisole have been identified long ago by UV hole burning spectroscopy[15] and in that work, the study of methanol–anisole was actually suggested. In the context of calibrating quantum-chemical methods for the description of polar *vs.* dispersive interactions of alcohols with ethers,[16] we found that the most reliable among the routinely applicable methods predict the two docking sites to be essentially isoenergetic for methanol–anisole, with at best a slight preference below 1 kJ mol^{-1} for the oxygen binding site. This has triggered a detailed supersonic jet study of the binary mixture, using a pulsed slit nozzle synchronized to the rapid scans of a FTIR spectrometer. As the isomerization barrier between the two docking sites is not very pronounced, one can expect a rather rigorous experimental ordering for the relative binding energies of the two isomers. This provides valuable benchmarks for theory, once the anharmonic nature of hydrogen bond interactions[17,18] is captured sufficiently well.

Beyond the relative binding energies of interest in the present work, absolute binding energy determinations for aromatic

Institut für Physikalische Chemie, Georg-August-Universität Göttingen, Tammannstr. 6, D-37077 Göttingen, Germany. E-mail: msuhm@gwdg.de

† Electronic supplementary information (ESI) available: Computed energetics and anharmonic constants of methanol–anisole, and binding energy of water–anisole. See DOI: 10.1039/c5cp01545f

complexes can be quite demanding.[2] The value derived for water–anisole from two-color dissociative photoionization is 15.4(5) kJ mol^{-1},[19] which may serve as a calibration value for the current investigation despite its large amplitude motion.[7] The present study forms the starting point of a systematic variation of the alcohol donor and ether acceptor molecules to map out the borderline between the OH–O and OH–π docking preference and compare the findings to high level and more approximate quantum chemical calculations.[20]

2 Methods

The technique used to generate cold methanol–anisole complexes has been described before.[21] They are formed transiently after the pulsed adiabatic expansion of the compound-loaded helium carrier gas through a 600 mm long slit nozzle into a large (>20 m^3) vacuum chamber. The size of the vacuum chamber prevents interactions of the expansion with background gas in the immediate neighborhood of the nozzle for a fraction of a second despite the limited pumping capacity (≈2500 m^3 h^{-1}). During this short time, full scans of an FTIR spectrometer (Bruker IFS 66v/S) at 2 cm^{-1} resolution (1.5 cm^{-1} in the OD case) are conducted through the adiabatic expansion using lenses. Feeble changes in the interferometrically modulated beam of a 150 W tungsten filament lamp are detected by a cooled 2 mm InSb or 3 mm InGaAs detector. Afterwards, the vacuum system recovers from the gas pulse for a time period of up to one minute. Scaling of the absorption features with concentration and pressure discriminates dimers from monomers and larger clusters. A comparison to single component expansions identifies mixed complexes. Linearity of the detection allows extraction of approximate relative intensities in different spectral ranges. Care is taken to correct for detector differences by reference measurements. Anisole and methanol are supplied to the carrier gas *via* temperature-controlled saturators. Overtone spectra are shown after linear baseline correction in the case of methanol–anisole.

Methanol (Roth, ≥99.9%), d1-methanol (euriso-top, 99% D), anisole (Fluka, >99%) and helium (Linde, 99.996%) were used as purchased. While this work is primarily spectroscopic in nature, the Gaussian09 Rev. D.01[22] and Turbomole 6.5[23,24] packages were used to obtain quantum-chemical predictions. Basis sets of the correlation-consistent family[25] (aug-cc-pVnZ, in short AVnZ) and the def2-TZVP basis set[26] are mostly used. When applying dispersion corrections (D3[27]), Becke–Johnson damping is always implied.[28] Small differences to zero-damping may be expected for the OH vibrational frequencies.[29]

3 Exploratory quantum chemical results

The size of the methanol–anisole complex and even somewhat larger systems allows for fairly rigorous *ab initio* electron correlation computations of the dissociation energy, which may be compared to dispersion-corrected double-hybrid[30] and hybrid density functional results.[27] The latter is rather useful for predictions of vibrational spectra and can thus also be employed for an estimate of the harmonic zero point energy, although some deficiencies for methanol OH stretching and librational modes have recently been noted.[31,32]

Table 1 Energy ΔE_0^h/(kJ mol^{-1}) of the OH–O-bound methanol–anisole complex relative to the OH–π-bound complex and its absolute dissociation energy D_0^h/(kJ mol^{-1}), as obtained for different combinations of the optimized structure and electronic (el.) energy combined with B3-D3 harmonic zero point energy, all employing triple zeta basis sets[a]

Structure	El. energy	ΔE_0^h/(kJ mol^{-1})	D_0^h/(kJ mol^{-1})
MP2	MP2	0.6	23.6
MP2	MP2-CP	0.5	17.4
B3-D3	B3-D3	−0.7	22.1
B3-D3	B3-D3-CP	−0.8	18.2
B2P-D3	B2P-D3	−1.1	19.1
SCS	SCS	0.1	18.7
B3-D3	CCSD(T)	−0.2	21.7
MP2	CCSD(T)	−0.1	21.5
B2P-D3	CCSD(T)	−0.3	21.7

[a] B3-D3 = B3LYP-D3/def2-TZVP, MP2 = MP2/AVTZ, B2P-D3 = B2PLYP-D3/AVTZ, CP = counterpoise correction, SCS = SCS-MP2/AVTZ, CCSD(T) = CCSD(T)/AVTZ.

Table 1 provides an overview of the results obtained by such size-scalable methods for triple-zeta basis sets, distinguishing between the electronic structure level used for structure optimization and the level used to compute the electronic energy, always estimating the zero-point energy difference of the competing complexes harmonically at the B3LYP-D3/def2-TZVP level. Relative energies of the O-bonded structures refer to the dissociation energy of the most stable π-bonded isomer, and the O-bonded absolute dissociation energies are listed explicitly in the last column (see also Tables S1–S3 in the ESI†).

We note that the role of (harmonically estimated) zero point energy is to favor the OH–π structure relative to OH–O by about 0.8 kJ mol^{-1} (B3LYP-D3/def2-TZVP, differing by 0.1 kJ mol^{-1} among a range of settings, see Table S2 in the ESI†). This is qualitatively reasonable, because OH–O hydrogen bonds are considerably more anisotropic, thus accumulating intermolecular zero point energy in their librational subspace.[32] We expect that the value could change by at most ±0.5 kJ mol^{-1} at higher levels of harmonic analysis. Taking this for granted, Table 1 suggests that π bonding is slightly favoured at the MP2 level, whereas O bonding is more favoured at the DFT levels. CCSD(T) calculations predict a perfectly balanced situation between the two docking sites, which is apparently only weakly dependent on the level used to obtain molecular structures.

One should also note that some of the fluctuations in the energy difference are comparable in size to some of the fluctuations in absolute binding energy. This suggests that the experimental investigation of such energy differences in the docking site provides useful benchmarks for theory, rather than being blurred by systematic error compensation. The two docking sites are sufficiently different in nature to turn the energy gap into a critical test for theory. Finally, the effects of counterpoise correction indicate that there is room for improvement in the basis set size although the table suggests that this is a less important issue for the energy difference of interest.

4 OH stretching fundamental results

If one assumes that the dominant peak in the OH fundamental spectrum at 3598 cm^{-1} (center trace of Fig. 1) is due to a single conformation of the mixed methanol–anisole dimer, its proximity to the methanol dimer absorption (MM) strongly indicates oxygen docking (MA_O). In line with expectations of an electron-deficient ether oxygen due to aromatic delocalization, the shift from the monomer (3686 cm^{-1}) is just 80% of that in the methanol dimer (3575 cm^{-1}). Towards 3620–3640 cm^{-1}, where OH–π docking would be expected to manifest itself,[33] only a very weak feature is observed (MA_π at 3629 cm^{-1}). Even when accounting for a reduced IR visibility of this weaker hydrogen bond by a factor of 2–3, we find that this minor component corresponds to about 20× lower abundance in the slit jet expansion. This translates into a ratio between the energy difference ΔE and RT_c of about 3, where T_c is the conformational temperature, *i.e.* the effective Boltzmann temperature where interconversion between the two docking sites freezes in the expansion. Estimates from calculations suggest an easily surmountable barrier between the docking motifs on the order of 3 kJ mol^{-1}. Even with a very low conformational temperature of 40 K (a more typical T_c value would be closer to 100 K[34]), one can still derive an energy penalty ΔE of at least 1 kJ mol^{-1} for the π docking site. More likely, this energy penalty is expected somewhere in the 1–2 kJ mol^{-1} range.

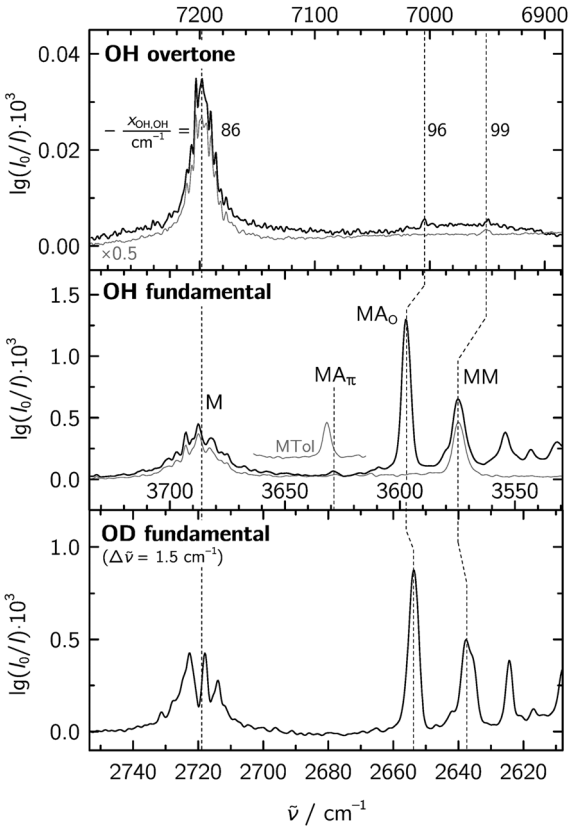

Fig. 1 Jet-FTIR spectra of a methanol–anisole (M–A) mixture in the monomer/dimer range for the OH stretching fundamental (center), the OH overtone (top) and the OD stretching fundamental of CH_3OD (bottom) compared to pure methanol reference expansions (grey, overtone from ref. 36). The top and bottom wavenumber scales are compressed (/2) and expanded ($\times\sqrt{2}$) after alignment of the monomeric M transition to emphasize changes in the dimer anharmonicity. Similar intensity and wavenumber scaling of mixed (MA) and pure methanol dimers (MM) reveals the O-bonded character of MA (central panel). Traces of π-bonded MA (further confirmed by a similar band in methanol–toluene, see the inset) essentially vanish upon deuteration (bottom panel) and are below the noise level in the overtone (top panel).

5 Towards possible explanations

There is thus a clear disagreement between standard quantum-chemical predictions and the experiment for the docking preference of methanol in the case of anisole. Harmonically zero-point corrected energy calculations predict an equivalence within 1 kJ mol^{-1} whereas the experimental spectra suggest a preference for the O docking by at least 1 kJ mol^{-1}. On the theoretical side, it may be that the structural predictions are inaccurate, the relative electronic energy could be biased towards π docking or the harmonic approximation might be insufficient for the zero-point energy difference. On the experimental side, only an accidental overlap of spectral transitions is conceivable as a qualitative error source, whereas extremely efficient interconversion between the two docking sites in the jet expansion would have to be invoked to explain the observed quantitative suppression of π docking despite a sub-kJ mol^{-1} energy difference.

We start with the experimental analysis, ruling out an accidental overlap of two conformations in the strong 3598 cm^{-1} signal attributed to the mixed dimer MA_O. An analogous experiment for CH_3OD also yields a single dominant mixed dimer band, as shown in the bottom trace of Fig. 1. Similar to the parent isotopologue, the shift from the monomer amounts to 80% of that of the methanol dimer. With a FWHM of 3.8 cm^{-1}, it is even more narrow than the parent transition (4.5 cm^{-1}). Persistent overlap is incompatible with this observation due to the significantly different anharmonic contributions in OH and OD stretching modes among the two docking sites.[35] The weak satellite band to higher wavenumbers (MA_π), which we tentatively assign to a minor OH–π contribution, is now even weaker. This meets the expectation that zero-point delocalization effects (which are more important for H than for D) tend to stabilize OH–π over OH–O, in agreement with the harmonic prediction. To further exclude that the dominant transition is mostly due to π docking, the OH overtone region was probed. There is only a single mixed dimer contribution above the noise level (upper trace in Fig. 1), from which an enhanced diagonal anharmonicity constant of −96 cm^{-1} compared to the methanol monomer value[35,36] of −86 cm^{-1} is derived. Furthermore, this overtone transition is attenuated by a factor of 500(150) relative to the fundamental (estimated error in parentheses), very characteristic of OH–O interactions. For comparison, the methanol dimer has an even larger diagonal anharmonicity constant of −99 cm^{-1} and a similarly high attenuation factor of 320(90) for its donor overtone.[36] If there was a significant OH–π contribution, it would show up prominently in the overtone region due to its smaller anharmonicity and much weaker attenuation of the intensity.

Another experimental piece of evidence against significant π docking is the dominant fundamental transition wavenumber itself (3598 cm^{-1}), which differs markedly from that of the methanol–benzene complex[33] (3639 cm^{-1}). Because it may be argued that the aromatic π system is more electron rich in anisole than in benzene, we have also recorded the spectrum of the methanol–toluene complex, obtaining an OH–π fundamental wavenumber of 3632 cm^{-1} (see the insert MTol in Fig. 1). This is still 34 cm^{-1} higher than the dominant methanol–anisole feature, but in very satisfactory agreement with the weak methanol–anisole band marked MA_π at 3629 cm^{-1}.

The observed discrepancy must therefore be due to the limited quality of most theoretical predictions listed in Table 1. A structural explanation may at first sight appear unlikely, as dispersion-corrected B3LYP calculations should capture the essence of both OH–O and OH–π interactions reasonably well and the CCSD(T) calculations predict essentially the same energy difference for all three optimized structures (Table 1). However, inspection of the corresponding OH–O structures (Fig. 2(a)) shows that the methyl group is positioned differently in the MP2-optimized structure. It interacts more closely with the benzene ring than in the two hybrid DFT structures, where the hydrogen bond is more structure-determining. In contrast, the most stable OH–π structure is rather similar across the three methods (Fig. 2(b)). To decide which of the OH–O structures is closer to reality, their electronic energy at the highest affordable level must be investigated and it will be shown below that the MP2-optimized OH–O structure is indeed more remote from the true structure. The calculations also reveal a second OH–π′ arrangement, which is more π-centered (Fig. 2(c), see also Table S4 in the ESI†). Although it is energetically higher than the OH–π structure shown in (b) at all investigated computational levels, it profits from a lower zero point energy and may fall within 1 kJ mol^{-1} of the more stable π structure. Inspection of its structure reveals that the OH–π′ configuration actually involves a more exclusive interaction with the π system, whereas the more stable structure additionally profits from two reciprocal methyl CH–O contacts in the 0.27–0.28 nm range. In the analogous toluene case (Fig. S11, and Tables S12 and S13 in the ESI†), where at least one of these contacts is lost, the two π-bonded structures become energetically nearly degenerate, but should still be spectrally distinguishable. The interaction potential between the OH group and the extended π system is generally expected to be relatively flat, possibly too flat to support the population of more than one of the connected potential wells in a supersonic jet expansion with its isomerising collisions. However, there is a sizeable statistical advantage for π-oriented structure formation associated with this, compared to the more narrow potential energy funnel offered by the oxygen atom in anisole. The fact that none of the two π structures is observed experimentally in methanol–anisole in significant abundance despite this statistical advantage points even more to a missing stabilization of OH–O at most computational levels summarized in Table 1.

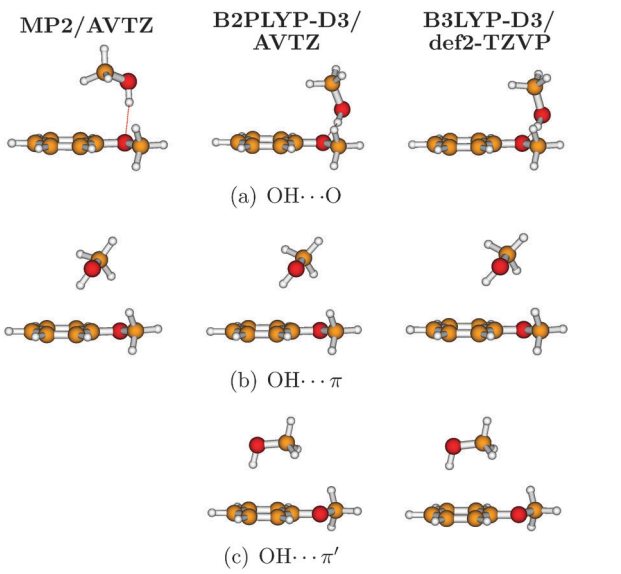

Fig. 2 Most stable methanol–anisole complexes optimized at three different levels. The MP2 OH–O structure (a) is seen to differ from the other by aligning the methyl group more closely to the π system. The most stable OH–π structure (b) shows one or two secondary aliphatic CH–O interactions. A second OH–π′ structure (c) positions the methanol primarily over the π system.

The second possible source of computational error refers to the electronic energy at the best structures. Table 1 includes calculations at the CCSD(T)/AVTZ level, considered to be reasonably accurate for absolute predictions and even more so for the relative energy prediction relevant to this work. It does indeed show a slight electronic preference for OH–O of 1.0 kJ mol^{-1}, but this is not enough to tip the balance towards OH–O docking after zero point energy correction. Counterpoise correction for the AVTZ basis set superposition error goes in a favorable direction for the energy difference, but is only on the order of 0.1 kJ mol^{-1} (Table 1) and thus insufficient to explain the discrepancy, even more so if one only includes 50% of this correction.[37] To further explore basis set incompleteness effects, we have thus extended the MP2-contribution to the AVQZ level. Surprisingly, this increases the relative MP2 stability of the OH–O structure by up to 1 kJ mol^{-1} (Table 2). Obviously, the two interaction sites show a very different basis set dependence. With the CCSD(T) correction on top, this means that the OH–O structure is now electronically up to 2.0 kJ mol^{-1} more stable than the most stable π complex. After harmonic zero point energy destabilization, this provides the first systematic *ab initio* prediction which is qualitatively compatible with experiment. We note that the somewhat less *ab initio* and much more economical double-hybrid approach (B2P-D3 in Table 2) is rather close. Even the B3-D3 hybrid functional prediction starts to overlap the experimental range, if optimization is performed using the AVTZ basis set instead of our standard def2-TZVP basis set. One may thus conclude that a correct balance between the O and π docking sites requires basis sets of quadruple-zeta quality for *ab initio* methods or at least AVTZ for hybrid DFT approaches. Furthermore, one can now judge the quality of the three structural predictions in Fig. 2 by applying the CCSD(T)-corrected MP2/AVQZ level to each of them. It turns out that the double hybrid structure yields the lowest OH–O and OH–π energies and is thus most likely the best relative structural prediction (see also Table S5 in the ESI†).

Table 2 Electronic energy ΔE_e/(kJ mol^{-1}) of the OH–O-bound methanol–anisole complex relative to the OH–π-bound complex and its absolute electronic dissociation energy D_e/(kJ mol^{-1}), as obtained for different combinations of the optimized structure and electronic energy. Also shown are selected relative electronic energies of the other OH–π′ complex $\Delta E_e'$/(kJ mol^{-1})[a]

Structure	Electronic energy	ΔE_e[b]	D_e	$\Delta E_e'$[c]
B3-D3	MP2/T	0.5	27.4	
MP2/T	MP2/T	−0.1	28.7	
B2P-D3	MP2/T	0.4	27.6	
B3-D3	B3-D3	−1.4	27.3	2.4
B3-D3/T	B3-D3/T	−1.9	24.2	1.3
B2P-D3	B2P-D3	−1.8	24.3	1.4
B3-D3	CCSD(T)	−1.0	26.8	
B2P-D3	CCSD(T)	−1.0	26.9	1.2
B3-D3	MP2/Q	−0.5	25.6	
MP2/T	MP2/Q	−0.5	25.9	
B2P-D3	MP2/Q	−0.6	25.7	0.7
B3-D3	MP2/Q + ΔCCSD(T)	−2.0	25.0	
MP2/T	MP2/Q + ΔCCSD(T)	−1.3	25.0	
B2P-D3	MP2/Q + ΔCCSD(T)	−2.0	25.0	1.3

[a] B3-D3 = B3LYP-D3/def2-TZVP, B3-D3/T = B3LYP-D3/AVTZ, B2P-D3 = B2PLYP-D3/AVTZ, MP2/T = MP2/AVTZ, MP2/Q = MP2/AVQZ, CCSD(T) = CCSD(T)/AVTZ, ΔCCSD(T) = (CCSD(T)-MP2)/AVTZ. [b] Add 1.0 kJ mol^{-1} for B3-D3/T harmonic zero point correction. [c] Subtract 0.6 kJ mol^{-1} for B3-D3/T harmonic zero point correction.

It is followed at a close distance by the B3LYP structure (with a balanced energy penalty of 0.3–0.4 kJ mol^{-1} for both docking sites), whereas the MP2/AVTZ structures are found to deviate by 0.9 kJ mol^{-1} for the OH–O site and by only 0.1 kJ mol^{-1} for the OH–π docking site. Clearly, the MP2/AVTZ approach provides an imbalanced structural description of the two methanol coordination options and should not be trusted for relative energy predictions. This parallels the overestimation of stacked aromatic interactions at the MP2 level.[38] Our best electronic prediction is thus that the OH–O structure is more stable than the OH–π structure by 2 kJ mol^{-1} and the second OH–π′ structure is less stable than OH–π by more than 1 kJ mol^{-1}.

Thirdly, the zero point energy correction itself needs to be addressed. As mentioned before, the B3-D3 approach predicts a harmonic advantage for OH–π of 0.8 kJ mol^{-1}. This is also basis set dependent, changing to 1.0 kJ mol^{-1} at the AVTZ level. On top of this harmonic uncertainty, one has to address anharmonic corrections. Even at the zero point level, anharmonicity effects on the order of 1–2% will persist, but most of those are expected to cancel for the difference between the two docking sites.[39] Unfortunately, vibrational perturbation treatments to include such effects[40–42] are not always reliable over the entire spectrum of normal modes for floppy systems.[43] While they provide fairly reliable high frequency mode corrections,[36] they occasionally tend to predict unphysical anharmonicity effects for large amplitude low frequency modes. In the present case, imaginary anharmonic frequencies were persistent for the OH–O and OH–π′ isomers. Therefore, we have to constrain the anharmonic analysis to the three most important differences between the docking sites, namely diagonal OH correction, torsional anharmonicity and OH–torsional coupling.[32] As shown in the ESI† (Table S7), the diagonal anharmonicity is more pronounced in the OH–O case, thus stabilizing the OH–O isomer. However, this correction amounts to less than 0.05 kJ mol^{-1} relative OH–O stabilization at the zero point level (B3LYP-D3/def2-TZVP, a level reproducing methanol and methanol dimer anharmonicities reasonably well,[36] see Table S7 in the ESI†). The methanol torsional mode acquires a significantly higher frequency in the OH–O case, a major reason for the total harmonic zero point energy stabilization of the OH–π docking site. If one trusts the vibrational perturbation theory analysis at least qualitatively and combines the effect of up to two modes with torsional character (see Table S8 in the ESI†), the diagonal anharmonic effect of torsion is to attenuate the zero point energy stabilization by less than 0.1 kJ mol^{-1}. The OH–torsional coupling is also more pronounced for OH–O docking and of similar size, but with opposite sign (ESI,† Table S8). This qualitatively counteracts the two diagonal terms, as observed in the methanol dimer OH stretching shift.[31] Indeed, one can expect that the net anharmonic effect on the zero point level difference between the two docking sites will be smaller than 0.1 kJ mol^{-1} and its net sign remains unclear. A converged full-dimensional anharmonic calculation of this effect would be desirable,[44] but so would be a further improved harmonic description. At the best available levels, zero point energy shrinks the predicted sequential energy spacing between the OH–O, OH–π and OH–π′ structures by a factor of two, to 1.1 and 0.7 kJ mol^{-1}, respectively. This is just in borderline agreement with our experimental interpretation.

A side effect of the anharmonic calculations is the OH overtone prediction, where vibrational perturbation theory has proved to be fairly reliable.[32] The predicted B3LYP-D3/def2-TZVP increase (in absolute value) of the anharmonicity constant in the OH–π complex amounts to 40% of that in the methanol dimer, whereas the observed increase is between 70 and 80% of the methanol dimer value, consistent with the predicted value for the OH–O complex of 71% (Table S7 in the ESI†). This provides further evidence for the OH–O structural assignment of the mixed dimer.

Another side effect of the anharmonic calculations is the availability of approximate fundamental/overtone intensity ratios for the donor OH stretching mode of methanol.[42] The perturbation theory results (Table S7 in the ESI†) confirm that the OH–O intensity ratio of methanol–anisole (300 at the B3LYP-D3/def2-TZVP level) is of the same order of magnitude as the methanol dimer (480, experimentally one finds 320(90)[36]), whereas for OH–π docking it is predicted below 100 and thus closer to the monomer (the monomer intensity ratio is predicted at only 5). Any OH–π fraction in the supersonic jet expansion should thus have an over-proportionally higher visibility in the overtone spectrum, but none is detected within the available signal-to-noise ratio. Quite in contrast, the observed intensity ratio of 500(150) is definitely too high to allow for significant OH–π contributions in the fundamental range, further reinforcing the experimental finding. This remains valid if a small part of the mixed dimer fundamental intensity stems from larger clusters in the concentrated expansion.

It is instructive to extract the actual D3 energy contributions to binding in the different complex isomers. At the B3LYP-D3 level, we find 12 kJ mol^{-1} dispersion energy gain for the OH–O

complex and 17–18 kJ mol^{-1} for the two OH–π complexes (see Table S6 in the ESI†). London dispersion interaction is seen to be a major stabilization force for OH–π docking, adding 50% to the dispersion contribution present in the O-bonded complex.

Expectedly somewhat less satisfactory is the predictive power of our quantum chemistry for the OH wavenumber difference between the two observed docking sites, experimentally indicated at 31 cm^{-1}. The B3-D3 harmonic prediction is 50 cm^{-1} (55 cm^{-1} for the AVTZ basis set), vibrational perturbation theory improves to 44 cm^{-1}, still 40% too high. Much of this deviation is to be blamed on the systematic overestimation of harmonic OH–O red shifts at all but the highest levels of electron correlation,[31] whereas OH–π shifts behave better.[29] As in similar cases,[45] monomer-shifted or -scaled harmonic predictions for the OH stretching fundamental slightly overestimate the absolute OH–π wavenumber (by 6 cm^{-1} at the B3-D3 level, but coincidentally 0 cm^{-1} with the AVTZ basis set) and underestimate the OH–O wavenumber (by 11 cm^{-1} at the B3-D3 level, but 22 cm^{-1} for the AVTZ basis set, see Table S7 in the ESI†).

Finally, we judge the reliability of the best calculated absolute dissociation energies by transferring our findings to the OH–O bonded water–anisole complex. The B2PLYP-D3/AVTZ optimized water–anisole structure (Fig. S9 in the ESI†) has an electronic dissociation energy relative to relaxed monomers of 21.9 kJ mol^{-1} at the MP2/AVQZ + ΔCCSD(T)/AVTZ level, which shrinks to 15.0 kJ mol^{-1} (15.1 kJ mol^{-1}) after including the harmonic B3LYP-D3/def2-TZVP (AVTZ) zero point energies (Table S10 in the ESI†). As anharmonic corrections are likely to increase this value slightly, agreement with the experimental value of 15.4(5) kJ mol^{-1} [19] could hardly be better. Thus, we can expect that not only energy differences but also absolute energies are quite accurate at this level. While the size-scalable consistent B3LYP-D3/def2-TZVP result expectedly overshoots (17.8 kJ mol^{-1}), B3LYP-D3/AVTZ (14.7 kJ mol^{-1}) is in line with the best value, as for methanol–anisole. We can therefore be confident that the zero-point-corrected dissociation energy of methanol–anisole in its preferred OH–O conformation is close to 20 kJ mol^{-1} and that the most stable OH–π conformation is at least 1 kJ mol^{-1} or 5% less stable.

6 Conclusions

By a combination of highly sensitive fundamental isotopologue and overtone spectroscopy of methanol–anisole mixtures in supersonic jet expansions, we firmly establish that the methanol molecule forms a hydrogen bond with the ether oxygen of anisole, whereas docking onto the π system is at least 1 kJ mol^{-1} less attractive and therefore hardly observable in the jet spectra.

A reasonably elaborate theoretical prediction including three independent structure optimizations, canonical CCSD(T)/AVTZ electronic energies, 50% MP2 counterpoise correction, harmonic B3LYP-D3/def2-TZVP zero-point energy correction and anharmonic estimates for off-diagonal and diagonal OH stretching contributions amounts to an energy penalty of about 0.4 kJ mol^{-1} for the OH–π structure. This is not quite sufficient to explain more than one order of magnitude less abundance in the supersonic jet expansion experiment, unless the conformational temperature was far lower than in other molecular systems. However, if we switch from AVTZ to an AVQZ basis set for the MP2 part, the OH–π structure is destabilized by another 1.0 kJ mol^{-1}, shifting theory into the experimentally compatible energy range. Similar results are obtained at the B3LYP-D3/AVTZ level and also at the B2PLYP-D3/AVTZ level, encouraging their use as workhorses for the prediction of energy preferences and spectra of a larger range of alcohol–ether complexes. Our results show that relative docking energies between O and π sites represent exquisitely sensitive testing cases for quantum chemical descriptions of weak to medium-strength hydrogen bonds. Due to the close energy balance, methodical variations cause qualitative changes and computational error compensation becomes unreliable as a consequence of the different nature of oxygen and π cloud docking. Higher level computational approaches[46,47] are invited to test our findings.

By subtle chemical modifications of the donor and/or acceptor (*e.g.* ring methylation), we expect to render OH–π docking slightly more attractive and thus clearly observable in supersonic jet expansions in competition with OH–O docking, even in the overtone range and also probing structural isotopic effects. This could turn the present single-sided experimental benchmark for hydrogen bond docking sites into a valuable double-sided benchmark at the sub-1 kJ mol^{-1} accuracy level.

Acknowledgements

This work was supported by the Deutsche Forschungsgemeinschaft (DFG, Grant SU 121/4) in preparation for the priority program SPP 1807 on control of dispersion interactions. It is dedicated to the memory of Bernhard Brutschy (†2014), a true pioneer in aromatic cluster spectroscopy. We thank Lars Biemann who recorded the first FTIR spectra of methanol–anisole complexes in the context of his undergraduate thesis (2004) and Hannes Gottschalk for help with reference measurements.

References

1 B. Brutschy and P. Hobza, Van der Waals molecules III: Introduction, *Chem. Rev.*, 2000, **100**, 3861–3862.
2 F. Lahmani, C. Lardeux-Dedonder, D. Solgadi and A. Zehnacker, Spectroscopic study of the anisole-benzene complex formed in a supersonic free jet, *J. Phys. Chem.*, 1989, **93**, 3984–3989.
3 H.-D. Barth, K. Buchhold, S. Djafari, B. Reimann, U. Lommatzsch and B. Brutschy, Hydrogen bonding in (substituted benzene)·(water)$_n$ clusters with $n < 4$, *Chem. Phys.*, 1998, **239**, 49–64.
4 B. Reimann, K. Buchhold, H.-D. Barth, B. Brutschy, P. Tarakeshwar and K. S. Kim, Anisole-$(H_2O)_n$ (n = 1–3) complexes: an experimental and theoretical investigation of the modulation of optimal structures, binding energies and vibrational spectra in both the ground and first excited states, *J. Chem. Phys.*, 2002, **117**, 8805–8822.

5 J. B. Nicholas and B. P. Hay, Anisole as an ambidentate ligand: *ab initio* molecular orbital study of alkali metal cations binding to anisole, *J. Phys. Chem. A*, 1999, **103**, 9815–9820.
6 M. Pasquini, N. Schiccheri, G. Piani, G. Pietraperzia, M. Becucci, M. Biczysko, M. Pavone and V. Barone, Isotopomeric conformational changes in the anisole-water complex: new insights from HR-UV spectroscopy and theoretical studies, *J. Phys. Chem. A*, 2007, **111**, 12363–12371.
7 B. M. Giuliano and W. Caminati, Isotopomeric conformational change in anisole-water, *Angew. Chem., Int. Ed.*, 2005, **44**, 603–606.
8 P. J. Breen, E. R. Bernstein, H. V. Secor and J. I. Seeman, Spectroscopic observation and geometry assignment of the minimum energy conformations of methoxy-substituted benzenes, *J. Am. Chem. Soc.*, 1989, **111**, 1958–1968.
9 G. Pietraperzia, M. Pasquini, F. Mazzoni, G. Piani, M. Becucci, M. Biczysko, D. Michalski, J. Bloino and V. Barone, Noncovalent interactions in the gas phase: the anisole-phenol complex, *J. Phys. Chem. A*, 2011, **115**, 9603–9611.
10 J. T. Yi, J. W. Ribblett and D. W. Pratt, Rotationally resolved electronic spectra of 1,2-dimethoxybenzene and the 1,2-dimethoxybenzene-water complex, *J. Phys. Chem. A*, 2005, **109**, 9456–9464.
11 S. Kumar, V. Pande and A. Das, π-hydrogen bonding wins over conventional hydrogen bonding interaction: a jet-cooled study of indole···furan heterodimer, *J. Phys. Chem. A*, 2012, **116**, 1368–1374.
12 H. Sasaki, S. Daicho, Y. Yamada and Y. Nibu, Comparable strength of OH–O *versus* OH–π hydrogen bonds in hydrogen-bonded 2,3-benzofuran clusters with water and methanol, *J. Phys. Chem. A*, 2013, **117**, 3183–3189.
13 L. J. H. Hoffmann, S. Marquardt, A. S. Gemechu and H. Baumgärtel, The absorption spectra of anisole-h8, anisole-d3 and anisole-d8. The assignment of fundamental vibrations in the S_0 and the S_1 states, *Phys. Chem. Chem. Phys.*, 2006, **8**, 2360–2377.
14 P. L. Raston, G. E. Douberly and W. Jäger, Single and double resonance spectroscopy of methanol embedded in superfluid helium nanodroplets, *J. Chem. Phys.*, 2014, **141**, 044301.
15 F. Lahmani and J. Sepiol, Spectral hole-burning isolation of fluorescent species in jet-cooled 9-methoxyanthracene complexes with water and alcohols, *Chem. Phys. Lett.*, 1992, **189**, 479–485.
16 M. A. Suhm, Hydrogen bond dynamics in alcohol clusters, *Adv. Chem. Phys.*, 2009, **142**, 1–57.
17 J. P. Perchard and Z. Mielke, Anharmonicity and hydrogen bonding I. A near-infrared study of methanol trapped in nitrogen and argon matrices, *Chem. Phys.*, 2001, **264**, 221–234.
18 T. Scharge, D. Luckhaus and M. A. Suhm, Observation and quantification of the hydrogen bond effect on O–H overtone intensities in an alcohol dimer, *Chem. Phys.*, 2008, **346**, 167–175.
19 M. Mons, I. Dimicoli and F. Piuzzi, Gas phase hydrogen-bonded complexes of aromatic molecules: photoionization and energetics, *Int. Rev. Phys. Chem.*, 2002, **21**, 101–135.
20 J. W. G. Bloom, R. K. Raju and S. E. Wheeler, Physical nature of substitution effects in XH/π interactions, *J. Chem. Theory Comput.*, 2012, **8**, 3167–3174.
21 M. A. Suhm and F. Kollipost, Femtisecond single-mole infrared spectroscopy of molecular clusters, *Phys. Chem. Chem. Phys.*, 2013, **15**, 10702–10721.
22 M. J. Frisch, G. W. Trucks, H. B. Schlegel, G. E. Scuseria, M. A. Robb, J. R. Cheeseman, G. Scalmani, V. Barone, B. Mennucci, G. A. Petersson, H. Nakatsuji, M. Caricato, X. Li, H. P. Hratchian, A. F. Izmaylov, J. Bloino, G. Zheng, J. L. Sonnenberg, M. Hada, M. Ehara, K. Toyota, R. Fukuda, J. Hasegawa, M. Ishida, T. Nakajima, Y. Honda, O. Kitao, H. Nakai, T. Vreven, J. A. Montgomery, Jr., J. E. Peralta, F. Ogliaro, M. Bearpark, J. J. Heyd, E. Brothers, K. N. Kudin, V. N. Staroverov, T. Keith, R. Kobayashi, J. Normand, K. Raghavachari, A. Rendell, J. C. Burant, S. S. Iyengar, J. Tomasi, M. Cossi, N. Rega, J. M. Millam, M. Klene, J. E. Knox, J. B. Cross, V. Bakken, C. Adamo, J. Jaramillo, R. Gomperts, R. E. Stratmann, O. Yazyev, A. J. Austin, R. Cammi, C. Pomelli, J. W. Ochterski, R. L. Martin, K. Morokuma, V. G. Zakrzewski, G. A. Voth, P. Salvador, J. J. Dannenberg, S. Dapprich, A. D. Daniels, O. Farkas, J. B. Foresman, J. V. Ortiz, J. Cioslowski and D. J. Fox, *Gaussian 09 Revision D.01*, Gaussian, Inc., Wallingford, CT, 2013.
23 R. Ahlrichs, M. Bär, M. Häser, H. Horn and C. Kölmel, Electronic structure calculations on workstation computers: the program system TURBOMOLE, *Chem. Phys. Lett.*, 1989, **162**, 165–169.
24 F. Furche, R. Ahlrichs, C. Hättig, W. Klopper, M. Sierka and F. Weigend, Turbomole, *Wiley Interdiscip. Rev.: Comput. Mol. Sci.*, 2014, **4**, 91–100.
25 R. A. Kendall, T. H. Dunning, Jr. and R. J. Harrison, Electron affinities of the first-row atoms revisited. Systematic basis sets and wave functions, *J. Chem. Phys.*, 1992, **96**, 6796–6806.
26 F. Weigend and R. Ahlrichs, Balanced basis sets of split valence, triple zeta valence and quadruple zeta valence quality for H to Rn: design and assessment of accuracy, *Phys. Chem. Chem. Phys.*, 2005, **7**, 3297–3305.
27 S. Grimme, J. Antony, S. Ehrlich and H. Krieg, A consistent and accurate *ab initio* parametrization of density functional dispersion correction (DFT-D) for the 94 elements H-Pu, *J. Chem. Phys.*, 2010, **132**, 154104.
28 S. Grimme, S. Ehrlich and L. Goerigk, Effect of the damping function in dispersion corrected density functional theory, *J. Comput. Chem.*, 2011, **32**, 1456–1465.
29 R. Medel, M. Heger and M. A. Suhm, Molecular docking *via* olefinic OH–π interactions: a bulky alkene model system and its cooperativity, *J. Phys. Chem. A*, 2015, **119**, 1723–1730.
30 S. Grimme, Semiempirical hybrid density functional with perturbative second-order correlation, *J. Chem. Phys.*, 2006, **124**, 034108.
31 M. Heger, M. A. Suhm and R. A. Mata, Communication: towards the binding energy and vibrational red shift of the simplest organic hydrogen bond: harmonic constraints for methanol dimer, *J. Chem. Phys.*, 2014, **141**, 101105.

32 F. Kollipost, J. Andersen, D. W. Mahler, J. Heimdal, M. Heger, M. A. Suhm and R. Wugt Larsen, The effect of hydrogen bonding on torsional dynamics: a combined far-infrared jet and matrix isolation study of methanol dimer, *J. Chem. Phys.*, 2014, **141**, 174314.
33 T. S. Zwier, The spectroscopy of solvation in hydrogen-bonded aromatic clusters, *Annu. Rev. Phys. Chem.*, 1996, **47**, 205–241.
34 N. O. B. Lüttschwager and M. A. Suhm, Stretching and folding of 2-nanometer hydrocarbon rods, *Soft Matter*, 2014, **10**, 4885–4901.
35 R. Wugt Larsen, P. Zielke and M. A. Suhm, Hydrogen-bonded OH stretching modes of methanol clusters: a combined IR and Raman isotopomer study, *J. Chem. Phys.*, 2007, **126**, 194307.
36 F. Kollipost, K. Papendorf, Y.-F. Lee, Y.-P. Lee and M. A. Suhm, Alcohol dimers - how much diagonal OH anharmonicity? *Phys. Chem. Chem. Phys.*, 2014, **16**, 15948–15956.
37 L. A. Burns, M. S. Marshall and C. David Sherrill, Comparing counterpoise-corrected, uncorrected and averaged binding energies for benchmarking noncovalent interactions, *J. Chem. Theory Comput.*, 2014, **10**, 49–57.
38 K. E. Riley, J. A. Platts, J. Řezáč, P. Hobza and J. Grant Hill, Assessment of the performance of MP2 and MP2 variants for the treatment of noncovalent interactions, *J. Phys. Chem. A*, 2012, **116**, 4159–4169.
39 M. Heger, K. E. Otto, R. A. Mata and M. A. Suhm, Bracketing subtle conformational energy differences between self-solvated and stretched trifluoropropanol, *Phys. Chem. Chem. Phys.*, 2015, **17**, 9899–9909.
40 G. Amat, H. H. Nielsen and G. Tarrago, *Rotation-Vibration of Polyatomic Molecules*, Marcel Dekker, N.Y., 1971.
41 V. Barone, Anharmonic vibrational properties by a fully automated second-order perturbative approach, *J. Chem. Phys.*, 2005, **122**, 014108.
42 J. Bloino and V. Barone, A second-order perturbation theory route to vibrational averages and transition properties of molecules: General formulation and application to infrared and vibrational circular dichroism spectroscopies, *J. Chem. Phys.*, 2012, **136**, 124108.
43 M. Umer and K. Leonhard, *Ab initio* calculations of thermochemical properties of methanol clusters, *J. Phys. Chem. A*, 2013, **117**, 1569–1582.
44 F. Pfeiffer, G. Rauhut, D. Feller and K. A. Peterson, Anharmonic zero point vibrational energies: tipping the scales in accurate thermochemistry calculations?, *J. Chem. Phys.*, 2013, **138**, 044311.
45 J. Altnöder, S. Oswald and M. A. Suhm, Phenyl- *vs* cyclohexyl-substitution in methanol: implications for the OH conformation and for dispersion-affected aggregation from vibrational spectra in supersonic Jets, *J. Phys. Chem. A*, 2014, **118**, 3266–3279.
46 J. M. Bowman, X. Huang, N. C. Handy and S. Carter, Vibrational levels of methanol calculated by the reaction path version of multimode, using an *ab initio*, full-dimensional potential, *J. Phys. Chem. A*, 2007, **111**, 7317–7321.
47 S. Kozuch, S. M. Bachrach and J. M. L. Martin, Conformational equilibria in butane-1,4-diol: a benchmark of a prototypical system with strong intramolecular H-bonds, *J. Phys. Chem. A*, 2014, **118**, 293–303.